Electronic Supplementary Material (ESI) for Dalton Transactions.
This journal is © The Royal Society of Chemistry 2023

Electronic Supporting Information

The gas-selective Zn-MOF exhibits selective sensing of Fe^{3+} ions by doping with Tb^{3+}

Zhi-Gang Wang,*[a,b] Tao Ding,[b] Jie Fei,*[a]

[a] *School of Materials, Northwestern Polytechnical University, Xi'an 710048, P. R China.*

[b] *School of Environmental and Chemical Engineering, Xi'an Polytechnic University, Xi'an 710048, P. R China.*

Table S1 Selected Bond Length (Å) and Angles (°) for Zn-MOF and Tb@Zn-MOF

Zn-MOF			
Zn(1)-O(3)#1	2.072(6)	Zn(1)-O(3)#2	2.072(6)
Zn(1)-O(5)#2	2.028(6)	Zn(1)-O(5)#1	2.028(6)
Zn(1)-N(1)	1.969(8)	Zn(2)-N(3)	1.998(6)
Zn(2)-N(6)#3	2.013(6)	Zn(2)-N(3)	1.998(6)
Zn(2)-O(7)	2.004(9)	Zn(2)-O(1)	2.004(9)
Zn(3)-O(4)	2.002(6)	Zn(3)-O(4)#4	2.002(6)
Zn(3)-O(6)	2.096(6)	Zn(3)-O(6)#4	2.096(6)
Zn(3)-N(4)	1.976(9)	O(5)#1-Zn(1)-O(3)#2	88.5(3)
O(5)#2-Zn(1)-O(3)#2	87.5(3)	O(5)#1-Zn(1)-O(3)#1	87.5(3)
O(5)#1-Zn(1)-O(3)#1	87.8(3)	O(5)#2-Zn(1)-O(3)#2	87.8(3)
O(5)#2-Zn(1)-O(3)#1	88.5(3)	O(5)#2-Zn(1)-O(5)#1	158.7(3)
N(1)-Zn(1)-O(3)#2	100.71(16)	N(1)-Zn(1)-O(3)#1	100.71(16)
N(1)-Zn(1)-O(5)#1	100.64(15)	N(1)-Zn(1)-O(5)#2	100.64(15)

N(3)-Zn(2)-N(6)#3	106.7(3)	N(3)-Zn(2)-O(1)	103.2(3)
N(3)-Zn(2)-O(7)	109.9(3)	O(1)-Zn(2)-N(6)#3	109.9(3)
O(1)-Zn(2)-O(7)	123.0(4)	O(7)-Zn(2)-N(6)#3	103.4(3)
O(4)-Zn(3)-O(6)#4	158.8(3)	O(4)#4-Zn(3)-O(6)	87.6(3)
O(4)-Zn(3)-O(6)#4	87.6(3)	O(4)#4-Zn(3)-O(6)#4	88.5(3)
O(4)-Zn(3)-O6	88.5(3)	O(6)#4-Zn(3)-O(6)	158.3(3)
N(4)-Zn(3)-O(4)#4	100.60(16)	N(4)-Zn(3)-O(4)	100.60(16)
N(4)-Zn(3)-O(6)	100.84(15)	N(4)-Zn(3)-O(6)#4	100.84(16)
Symmetrical codes: #1 -x+1/2,-y+3/2,-z+1/2;#2 x-1/2,y,-z+1/2;#3 x-1/2,-y+3/2,-z+1;#4 -x+1,-y+3/2,z+0;#5 -x+0,-y+3/2,z+0;#6 -x+1/2,y-1/2,z;#7 x+1/2,-y+3/2,-z+1;#8 -x+1/2,y+1/2,z.			
Tb@Zn-MOF			
N(4)-Zn(1)	1.982(4)	N(5)-Zn(2)	1.983(6)
O(1)-Zn(1)	1.948(5)	O(4)-Zn(2)#2	2.058(4)
O(5)-Zn(2)#3	2.045(4)	O(1)#6-Zn(1)-O(1)	109.4(3)
O(1)#6-Zn(1)-N(4)	102.46(19)	O(1)-Zn(1)-N(4)	116.5(2)
O(1)#6-Zn(1)-N(4)#6	116.5(2)	O(1)-Zn(1)-N(4)#6	102.47(19)
N(4)-Zn(1)-N(4)#6	110.1(3)	N(5)-Zn(2)-O(5)#7	107.14(19)
N(5)-Zn(2)-O(5)#8	107.14(19)	O(5)#7-Zn(2)-O(5)#8	86.4(3)
O(5)#7-Zn(2)-O(4)#2	156.83(18)	O(5)#8-Zn(2)-O(4)#2	88.3(2)
N(5)-Zn(2)-O(4)#9	95.98(19)	O(5)#7-Zn(2)-O(4)#9	88.3(2)
O(5)#8-Zn(2)-O(4)#9	156.83(18)	O(4)#2-Zn(2)-O(4)#9	87.7(3)
Symmetry codes: #1 x,-y+1,z;#2 -x+3/2,-y+3/2,-z+1;#3 x+1/2,y+1/2,z+1;#4-x+1,-y+1,-z;#5 x,-y+2,z;#6 -x+1,y,-z+1;#7 x-1/2,y-1/2,z-1;#8 x-1/2,-y+3/2,z-1;#9 -x+3/2,y-1/2,-z+1.			

Table S2 Results of the ICP-OES analyses obtained for **Tb@Zn-MOF**

Test element	Sample quality (g)	C_0 (mg/L)	Sample element content C_x (mg/kg)	Sample element content W (%)
Tb	0.1154	1.841	3988	0.40
Zn	0.1154	5.897	12774	1.28

Table S3 Results of the EDS analyses obtained for **Tb@Zn-MOF**

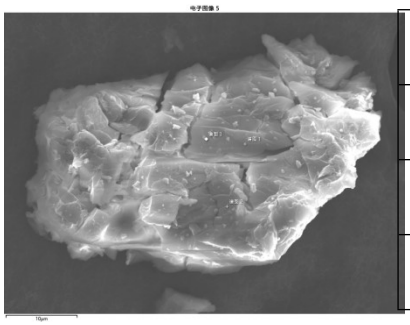

	Graph 1	Graph 2	Graph 3
Element	W_t (%)		
Zn	25.81	33.66	32.89
Tb	0.35	1.01	1.39

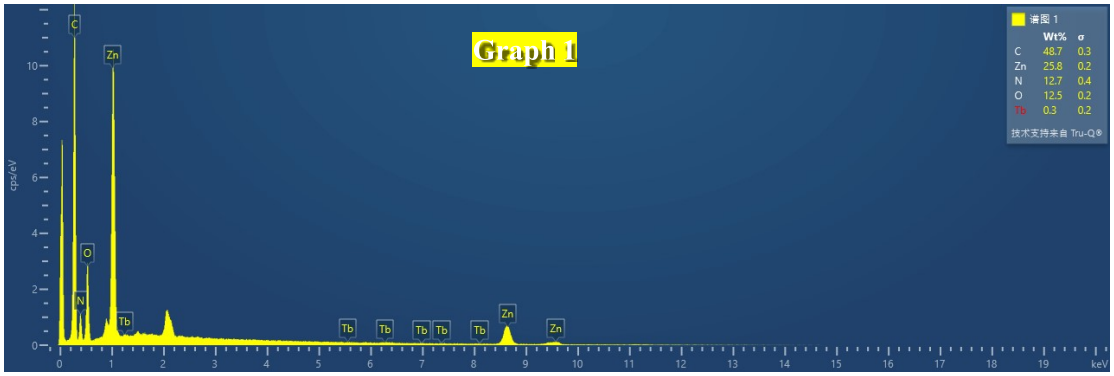

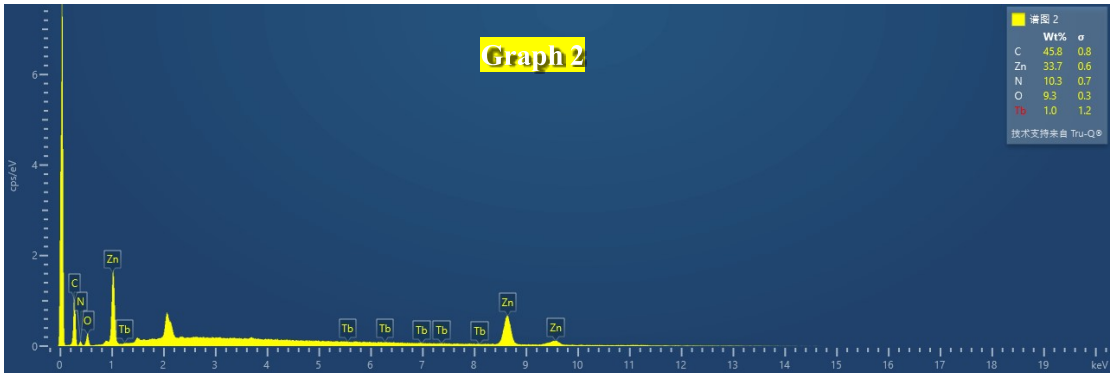

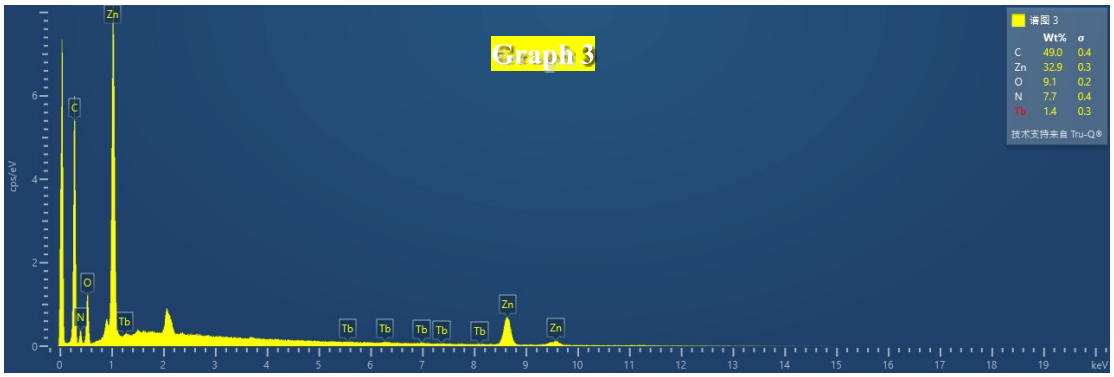

Table S4 A comparison of various MOFs materials used for selective adsorption for C_2H_2 and CO_2 over CH_4.

MOFs materials	IAST calculated selectivity		Ref.
	C_2H_2/CH_4	CO_2/CH_4	
ZJNU-98		5.7	1b
ZJNU-81		5.46	2b
Zn-MOF	11.87	8.18	5a
$\{[Co_3(L)(OH)_2(H_2O)_4]\cdot 2DMF\cdot 2H_2O\}_n$	13	4	9
$\{[Cu_4(L)_2(H_2O)_4]\cdot 4DMF\cdot 8H_2O\}_n$		3.2	13a
$[(CH_3)_2NH_2][Zn_{1.5}(\mu_3\text{-}O)_{0.5}(F\text{-}tzba)_{1.25}(bpy)_{0.25}(\mu_2\text{-}F)_{0.5}]\cdot 2DMF\cdot 2H_2O$	14.4	4.2	14a
ZJNU-63	13.1	3.5	14b
$\{[Co_6(\mu 3\text{-}OH)4(Ina)_8](H_2O)_{10}(DMA)_2\}_n$	9.6		14c
ZJU-16a	7.5		14d
MOF-505	~8.9		15a
$Zn_2(TCPP)(DPB)$	12.1		15b
SNNU-5-In	10	3.9	15c

Zn-MOF	14.48	6.04	This work

Table S5 Comparison the K_{sv} of **Tb@Zn-MOF** towards Fe^{3+} with other materials

MOFs materials	K_{sv} (M^{-1})	Ref.
$H_3O[In_3(dcpy)_4(OH)_2]\cdot 3DMF\cdot 4H_2O$	4.3×10^3	5b
Eu-MOF	1.78×10^4	5d
Tb(3+)@Zn-MOF	1.57×10^4	8b
Zn-MOF	1.9×10^4	16b
Tb-DSOA	3.54×10^3	17a
$[Tb_4(L)_6(H_2O)_8]$	1.88×10^4	17b
534-MOF-Tb	5.51×10^3	17c
Tb-N	7.93×10^3	19
Tb-F	1.39×10^4	19
Tb@Zn-MOF	2.79×10^4	This work

Fig. S1 The L^{4-} ligand viewed as two 3-c nodes.

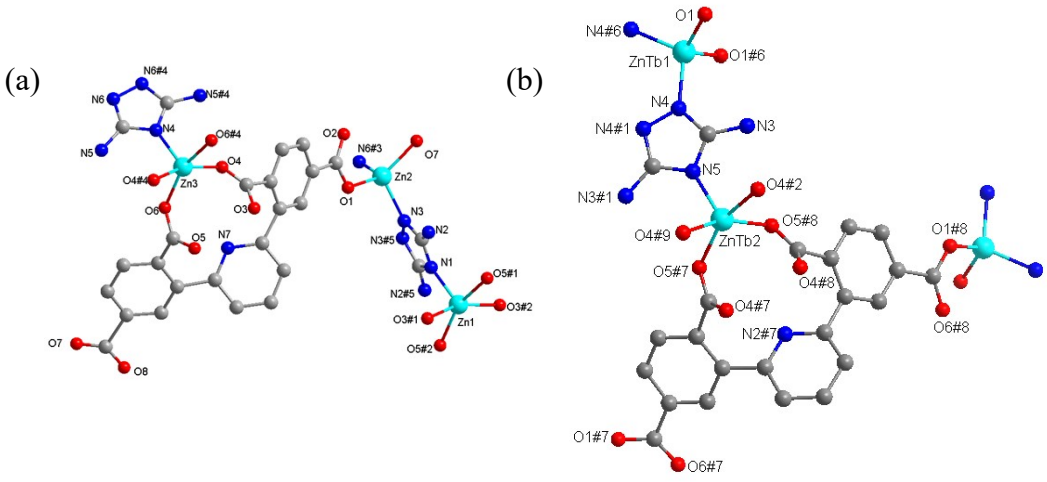

Fig. S2 Coordination environments of **Zn-MOF** (a) and **Tb@Zn-MOF** (b).

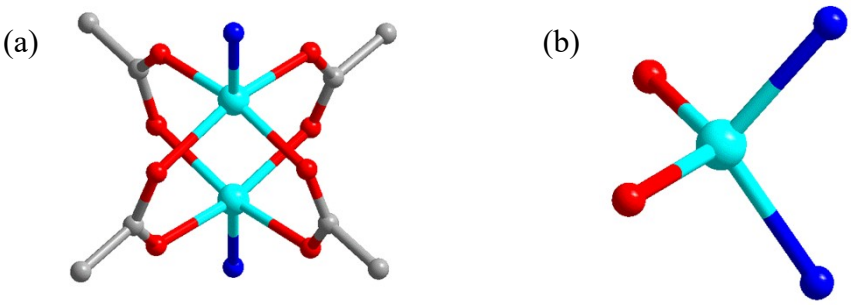

Fig. S3 $[Zn_2(COO)_4(N)_2]$ cluster (a) and ZnO_2N_2 cluster (b).

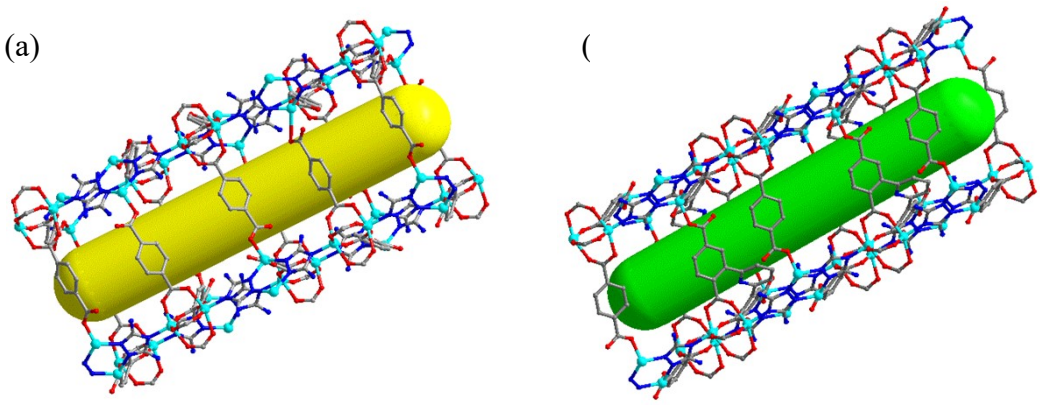

Fig. S4 The channel of **Zn-MOF** (a) and **Tb@Zn-MOF** (b).

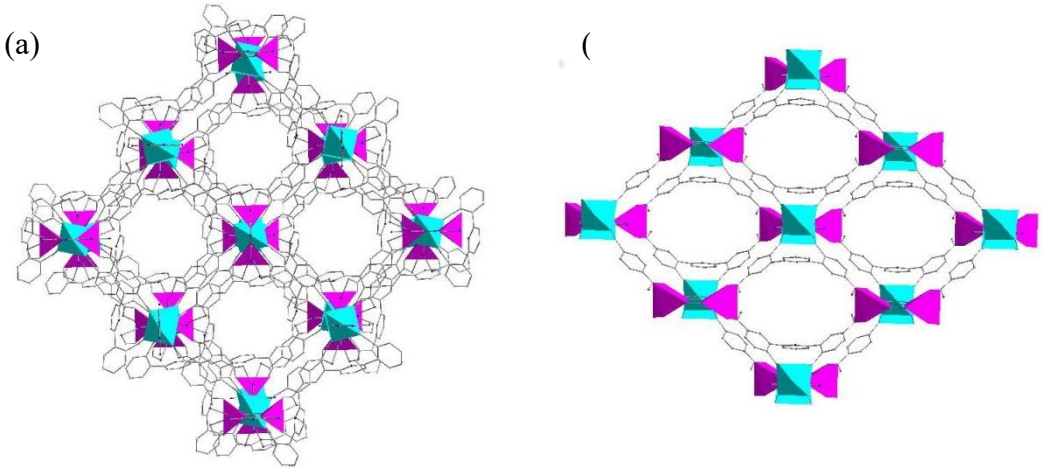

Fig. S5 The four alternately connected layers in **Zn-MOF** (a) and the two alternately connected layers in **Tb@Zn-MOF** (b).

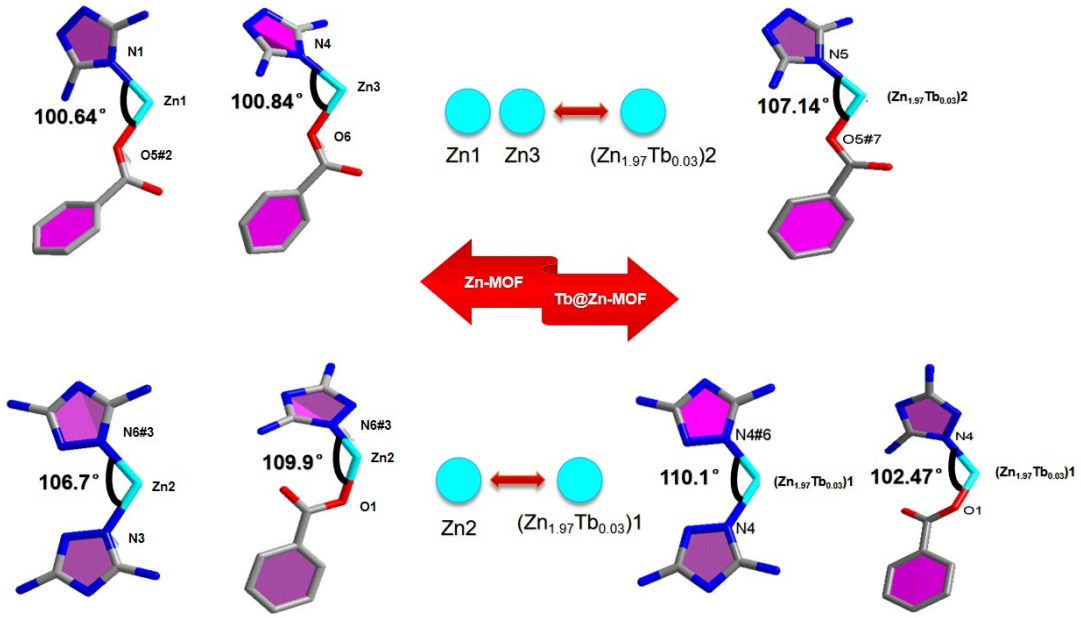

Fig. S6 Coordination angles of Zn(II) ions in **Zn-MOF** and **Tb@Zn-MOF**.

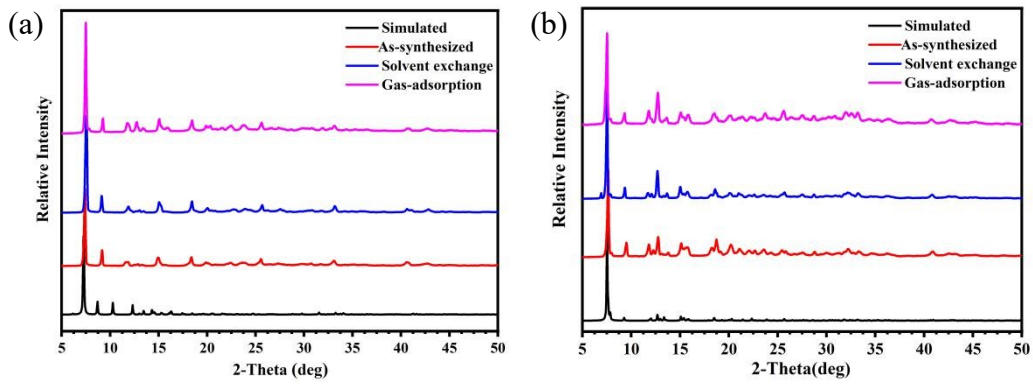

Fig. S7 PXRD patterns for **Zn-MOF** (a), **Tb@Zn-MOF** (b)：Simulated, as-synthesized,solvent exchange and gas-adsportion samples.

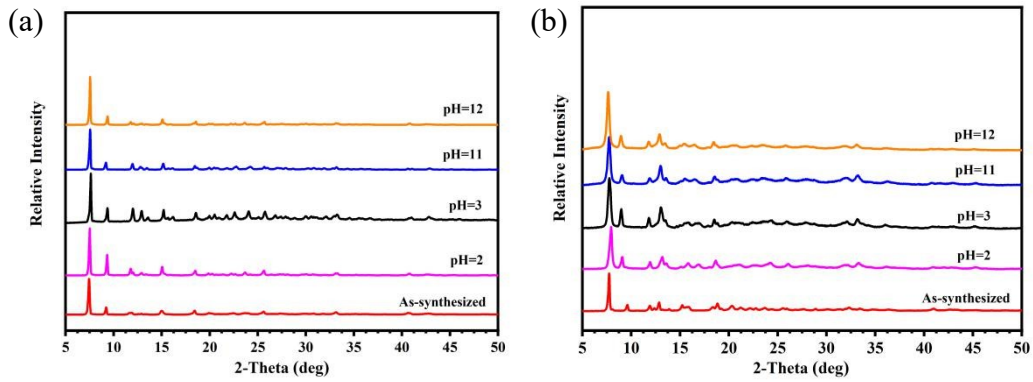

Fig. S8 PXRD patterns for **Zn-MOF** (a), **Tb@Zn-MOF** (b) after being soaked in acidic and basic solutions.

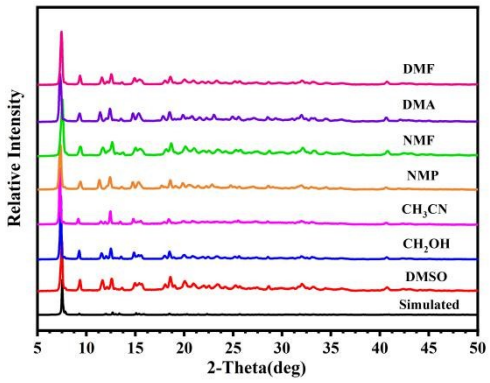

Fig. S9 PXRD patterns for **Tb@Zn-MOF** after being soaked in different organic solvents.

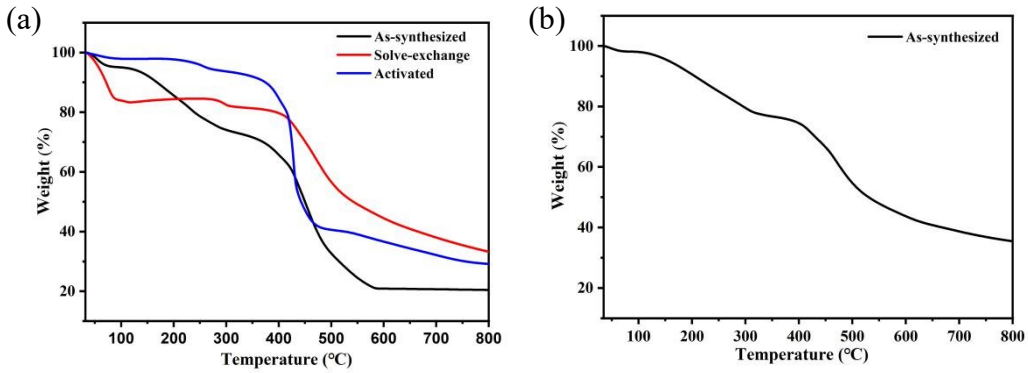

Fig. S10 TGA for **Zn-MOF** (a) and **Tb@Zn-MOF** (b).

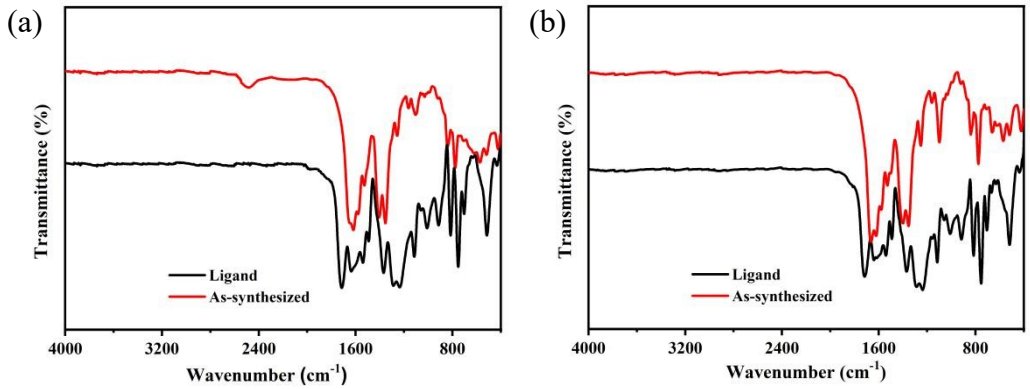

Fig. S11 IR for ligand and as-synthesized samples: **Zn-MOF** (a) and **Tb@Zn-MOF** (b).

IAST adsorption selectivity calculation

The experimental isotherm data for pure C_2H_2, CO_2 and CH_4 (measured at 298 K) were fitted using a Langmuir-Freundlich (L-F) model

$$q = \frac{a * b * p^c}{1 + b * p^c}$$

Where q and p are adsorbed amounts and pressures of component i, respectively. The adsorption selectivities for binary mixtures of C_2H_2/CH_4 and CO_2/CH_4, defined by

$$S_{i/j} = \frac{(x_i * y_j)}{(x_j * y_i)}$$

were calculated using the Ideal Adsorption Solution Theory (IAST) of Myers and Prausnitz.

Where x_i the mole fraction of component i in the adsorbed phase and y_i is the mole fraction of component i in the bulk.

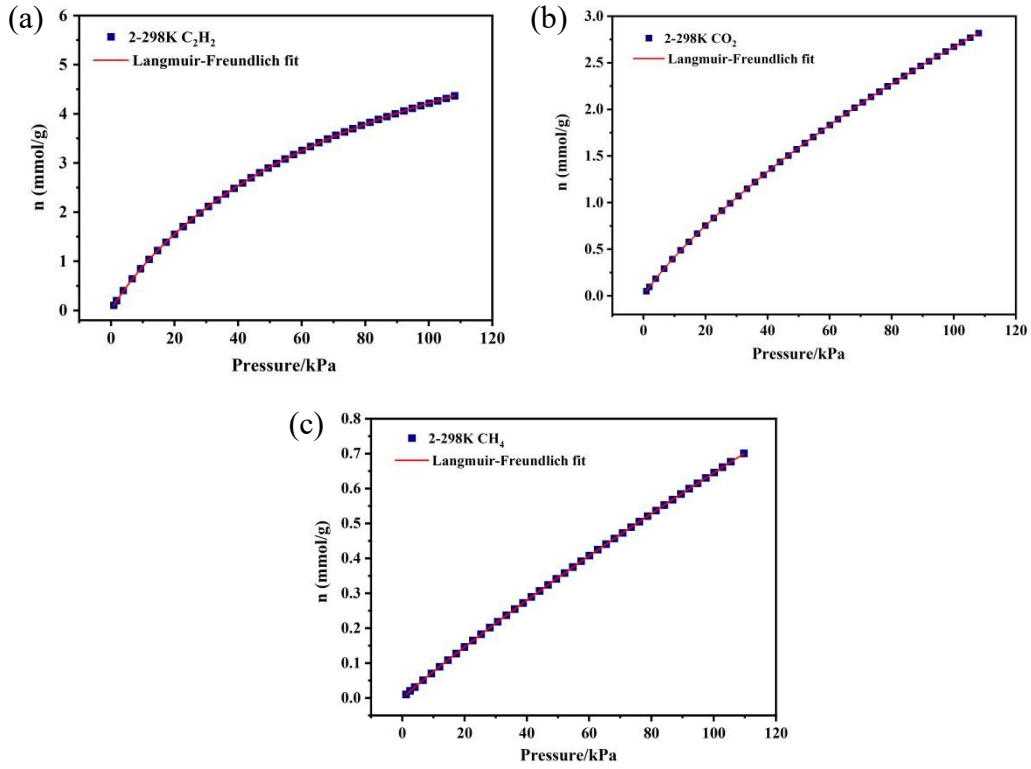

Fig. S12 (a) C_2H_2 adsorption isotherms of **Zn-MOF** at 298 K with fitting by L-F model: a =8.248, b =0.014, c =0.084, Chi^2 = 6.2E-5, R^2 = 0.99999; (b) CO_2 adsorption isotherms of **Zn-MOF** at 298 K with fitting by L-F model: a =12.59506, b =0.0043, c =0.102, Chi^2 =3.2E-7, R^2 = 1; (c) CH_4 adsorption isotherms of **Zn-MOF** at 298 K with fitting by L-F model: a = 7.83267, b =0.00106, c =0.03594, Chi^2 = 2.6E-5, R^2 =1.

Calculation of sorption heat for C_2H_2 and CO_2 uptakes using Virial 2 model

The above equation was applied to fit the combined C_2H_2 and CO_2 and isotherm data

for desolvated **1a** at 273 and 298 K, where *P* is the pressure, *N* is the adsorbed amount, *T* is the temperature, *ai* and *bi* are virial coefficients, and *m* and *n* are the number of coefficients used to describe the isotherms. Q_{st} is the coverage-dependent enthalpy of adsorption and *R* is the universal gas constant.

$$\ln P = \ln N + 1/T \sum_{i=0}^{m} aiN^i + \sum_{i=0}^{n} biN^i Q_{st} = -R \sum_{i=0}^{m} aiN^i$$

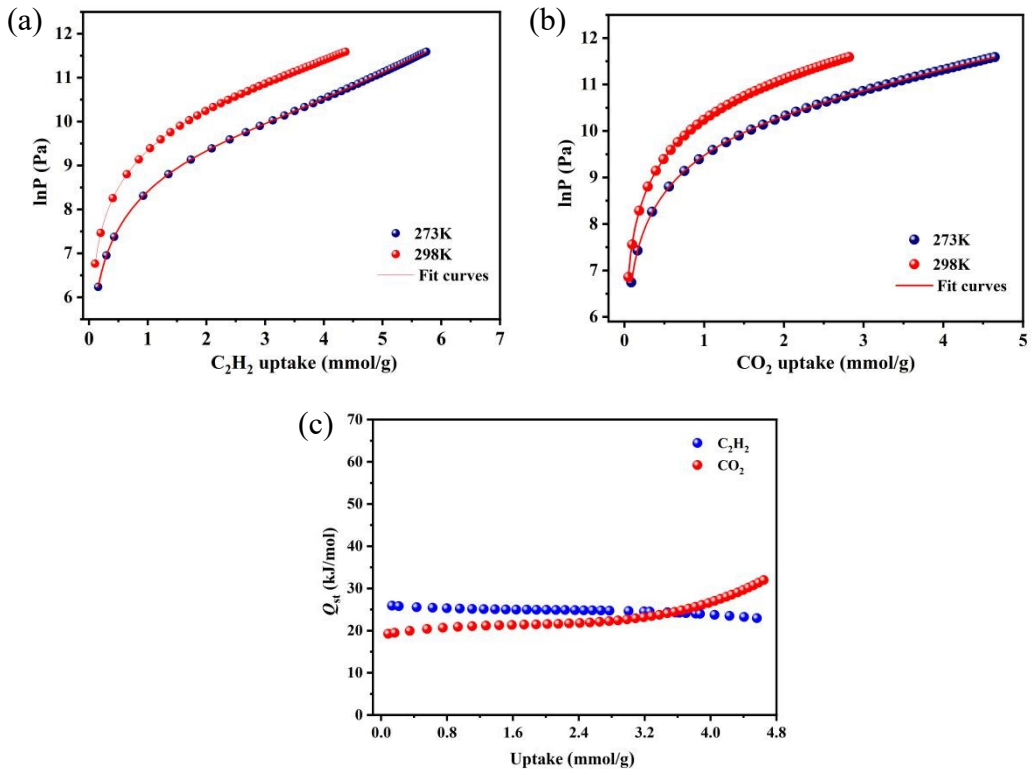

Fig. S13 (a) Virial analysis of the C_2H_2 adsorption data at 298 K and 273 K for **Zn-MOF**. Fitting results: a0= -3136.8988, a1 = 178.38107, a2 = -85.06356, a3 = 16.75777, a4 = -0.59305, b0 = 19.51637, b1 = -0.1369, b2 = 0.14452, b3 = -0.02591, Chi^2 = 8.14263E-6, R^2 = 0.99999; (b) Virial analysis of the CO_2 adsorption data at 298 K and 273 K for **Zn-MOF**. Fitting results: a0= -2282.40823, a1 = -400.37189, a2 = 196.78851, a3 = -34.39808, a4 = -1.0745, b0 = 17.53214, b1 =1.9186, b2 = -0.91172, b3 = 0.17317, Chi^2 = 4.32643E-5, R^2 = 0.99996; (c) Isosteric heat of C_2H_2 and CO_2 in **Zn-MOF**.

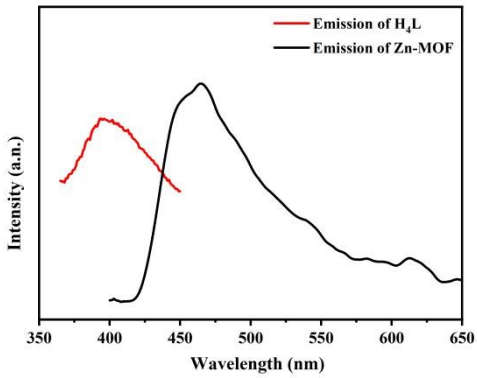

Fig. S14 The solid-state luminescence spectra of the H_4L ligand and **Zn-MOF**.

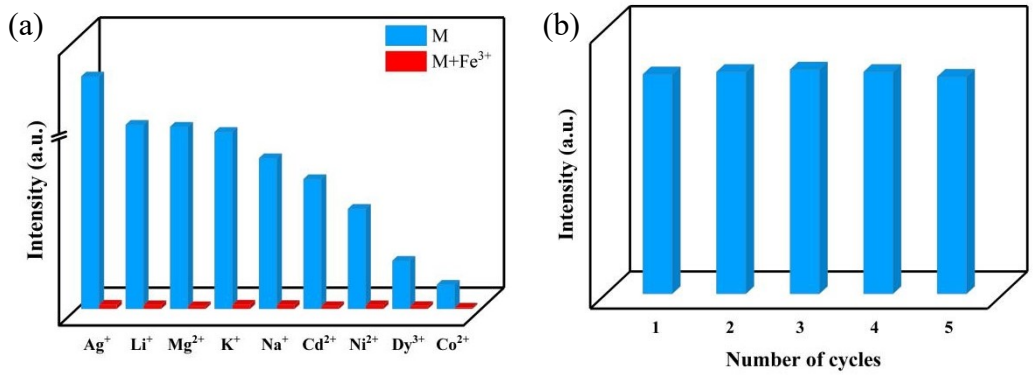

Fig. S15 (a) Luminescence intensities of **Tb@Zn-MOF** in different mixed metal solutions; (b) Multiple cycles for the luminescence quenching of **Tb@Zn-MOF** toward Fe^{3+} and recovery after washing by H_2O for several times.

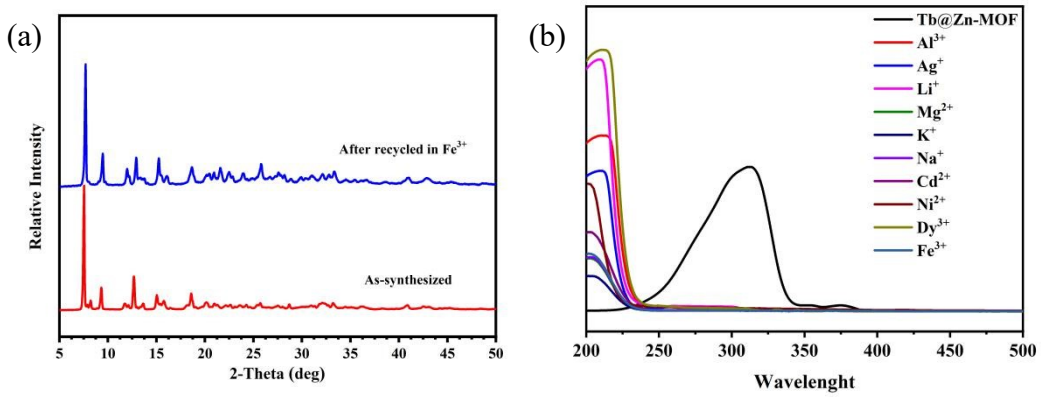

Fig. S16 (a) PXRD patterns and (b) UV-vis adsorption spectra of $M(NO_3)_x$ aqueous and the excitation spectrum of **Tb@Zn-MOF**.

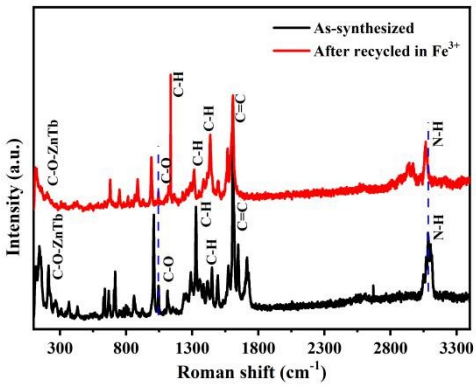

Fig. S17 Raman spectra of **Tb@Zn-MOF** before and after treatment of Fe^{3+}.